Kullaa, Jyrki (2019). Structural Health Monitoring using a Large Sensor Network and Bayesian Virtual Sensors. *Advances in Signal Processing and Artificial Intelligence. Proceedings of the 1st International Conference on Advances in Signal Processing and Artificial Intelligence. 20-21 March 2019 Barcelona, Spain,* 13-17. IFSA Publishing.

Oral

Topic: Sensor Array and Multichannel Signal Processing

Structural Health Monitoring using a Large Sensor Network and Bayesian Virtual Sensors

J. Kullaa

Metropolia University of Applied Sciences, Department of Automotive and Mechanical Engineering,
P.O. Box 4071, 00079 Metropolia, Finland
Tel.: +358 40 3340429
E-mail: jyrki.kullaa@metropolia.fi

Summary: Damage detection in structural health monitoring is based on unsupervised learning. Training data consist of multichannel vibration measurements of the undamaged structure under different environmental or operational conditions. The excitation (input) and the environmental or operational variables are usually unknown, but noisy response is only measured. In subsequent data analyses, the noisy measurements are replaced by Bayesian virtual sensors that are more accurate than the corresponding hardware. Environmental or operational variability between measurements can be taken into account using the minimum mean square error (MMSE) estimation. Damage detection is done in the time domain using statistical analysis including residual generation, principal component analysis, and an extreme value statistics control chart. A numerical experiment is performed for a bridge structure having a crack with different sizes. Virtual sensors outperformed the raw measurements in damage detection and damage was correctly localized to the nearest sensor.

Keywords: Virtual sensing, Structural health monitoring, Novelty detection, Bayes' rule, Vibration measurements, Sensor array, Estimation.

1. Introduction

Large structures like bridges or other important infrastructure can be monitored for an early detection of faults. Structural health monitoring (SHM) can be based on vibration measurements, which is attractive, because it is global, i.e. damage can be detected remotely from the sensor. However, in order to have an early warning, the monitoring system must be sensitive to small changes and insensitive to varying environmental or operational conditions. A small measurement error and statistical data analysis of multivariate vibration records are therefore necessary.

If a sufficiently large sensor array is installed on the structure, the system is redundant. This hardware redundancy can be used to compensate for the environmental or operational influences and reduce measurement errors using virtual sensing techniques.

The paper is organized as follows. Bayesian virtual sensing is introduced in Section 2 resulting in virtual sensors that are more accurate than the hardware. Section 3 is devoted to a damage detection algorithm capable of eliminating environmental or operational influences. Numerical simulations of a bridge under random excitation, environmental variability, and damage are performed in Section 4. Damage detection is done using the actual measurements or the virtual sensors. Finally, concluding remarks are presented in Section 5.

2. Bayesian Virtual Sensing

Virtual sensing (VS) gives an estimate of a quantity of interest using the available measurements. Empirical VS is a data-based approach, estimating a physical sensor using hardware redundancy. In structural vibrations of linear structures, the response can be written as a contribution of natural modes:

$$\mathbf{x}(t) = \mathbf{\Phi q}(t) = \sum_{i=1}^{N} \phi_i q_i(t) \approx \sum_{i=1}^{n} \phi_i q_i(t) \quad (1)$$

where $\mathbf{x}(t)$ is the displacement response, N is the number of DOF in the finite element model, $n << N$ is the selected number of modes, Φ is the modal matrix consisting of the mode shapes ϕ_i as columns, and $\mathbf{q}(t)$ are the modal or generalized coordinates. The last expression in (1) suggests that the response can be expressed with sufficient accuracy by including only the lowest n modes. In the case of SHM, the excitation is due to wind, waves, traffic, or micro-tremors having a narrow bandwidth. Therefore, the n lowest modes are usually able to describe the vibration response of the structure. Consequently, more than n sensors are needed to make the sensor network redundant.

Virtual sensing techniques can be used to obtain an estimate for each sensor, which is more accurate than the corresponding hardware.

Consider a sensor network measuring p simultaneously sampled variables $\mathbf{y} = \mathbf{y}(t)$ at time t. Each measurement $\mathbf{y}$ includes independent measurement error $\mathbf{w} = \mathbf{w}(t)$:

$$\mathbf{y} = \mathbf{x} + \mathbf{w} \quad (2)$$

where $\mathbf{x} = \mathbf{x}(t)$ are the true values of the measured degrees of freedom. The objective is to find an estimate for the true values $\mathbf{x}$ utilizing the noisy measurements $\mathbf{y}$.

In a sensor array, a true reading for sensor u, x_u, can be estimated using the noisy measurements $\mathbf{y}$ by conditioning on the remaining sensors v and applying Bayes' rule [1]. The partitioned variables are

$$\mathbf{y} = \begin{Bmatrix} \mathbf{y}_u \\ \mathbf{y}_v \end{Bmatrix}, \ \mathbf{x} = \begin{Bmatrix} \mathbf{x}_u \\ \mathbf{x}_v \end{Bmatrix}, \ \mathbf{w} = \begin{Bmatrix} \mathbf{w}_u \\ \mathbf{w}_v \end{Bmatrix} \quad (3)$$

The measurement error $\mathbf{w}$ is assumed to be zero mean, independent of $\mathbf{x}$, with a known covariance matrix

$$\mathbf{\Sigma}_w = E(\mathbf{w}\mathbf{w}^T) = \begin{bmatrix} \mathbf{\Sigma}_{w,uu} & \mathbf{\Sigma}_{w,uv} \\ \mathbf{\Sigma}_{w,vu} & \mathbf{\Sigma}_{w,vv} \end{bmatrix} \quad (4)$$

where $E(\cdot)$ denotes the expectation operator. After partitioning, all distributions are conditioned with $\mathbf{y}_v$. Bayes' rule becomes

$$\begin{aligned} p(\mathbf{x}_u \mid \mathbf{y}) &= p(\mathbf{x}_u \mid \mathbf{y}_u, \mathbf{y}_v) \\ &= \frac{p(\mathbf{y}_u \mid \mathbf{x}_u, \mathbf{y}_v)\, p(\mathbf{x}_u \mid \mathbf{y}_v)}{p(\mathbf{y}_u \mid \mathbf{y}_v)} \\ &= \frac{p(\mathbf{y}_u \mid \mathbf{x}_u)\, p(\mathbf{x}_u \mid \mathbf{y}_v)}{p(\mathbf{y}_u \mid \mathbf{y}_v)} \end{aligned} \quad (5)$$

The distributions in (5) can be evaluated as shown in the following.

2.1. Likelihood

Assuming Gaussian noise $\mathbf{w}$, the likelihood is obtained using Equation 2:

$$\begin{aligned} p(\mathbf{y}_u \mid \mathbf{x}_u) &= N(\mathbf{y}_u \mid \mathbf{x}_u, \mathbf{\Sigma}_{w,uu}) \\ &\propto \exp\left[-\frac{1}{2} (\mathbf{y}_u - \mathbf{x}_u)^T \mathbf{\Sigma}_{w,uu}^{-1} (\mathbf{y}_u - \mathbf{x}_u) \right] \end{aligned} \quad (6)$$

2.2. Evidence

For simplicity but without loss of generality, assume zero-mean variables $\mathbf{y}$. The partitioned data covariance matrix $\mathbf{\Sigma}_y$ is

$$\mathbf{\Sigma}_y = E(\mathbf{y}\mathbf{y}^T) = \begin{bmatrix} \mathbf{\Sigma}_{y,uu} & \mathbf{\Sigma}_{y,uv} \\ \mathbf{\Sigma}_{y,vu} & \mathbf{\Sigma}_{y,vv} \end{bmatrix} \quad (7)$$

The precision matrix $\mathbf{\Gamma}_y$ is defined as the inverse of the covariance matrix $\mathbf{\Sigma}_y$ and is also written in a partitioned form:

$$\mathbf{\Gamma}_y = \mathbf{\Sigma}_y^{-1} = \begin{bmatrix} \mathbf{\Gamma}_{y,uu} & \mathbf{\Gamma}_{y,uv} \\ \mathbf{\Gamma}_{y,vu} & \mathbf{\Gamma}_{y,vv} \end{bmatrix} \quad (8)$$

A linear minimum mean square error (LMMSE) estimate for $\mathbf{y}_u \mid \mathbf{y}_v$ is obtained by minimizing the mean-square error (MSE) and can be computed either using the covariance or precision matrix [2, 3]. If each sensor signal is estimated in turn, the formulas based on the precision matrix result in a more efficient algorithm [2]. The expected value of the estimated variable is:

$$\hat{\mathbf{y}}_u = E(\mathbf{y}_u \mid \mathbf{y}_v) = -\mathbf{\Gamma}_{y,uu}^{-1} \mathbf{\Gamma}_{y,uv} \mathbf{y}_v = \mathbf{K}\mathbf{y}_v \quad (9)$$

where $\mathbf{K} = -\mathbf{\Gamma}_{y,uu}^{-1} \mathbf{\Gamma}_{y,uv}$, and the MSE is

$$\operatorname{cov}(\mathbf{y}_u \mid \mathbf{y}_v) = \mathbf{\Gamma}_{y,uu}^{-1} \quad (10)$$

The evidence $p(\mathbf{y}_u \mid \mathbf{y}_v)$ is also Gaussian with the mean and covariance from Equations (9) and (10), respectively:

$$\begin{aligned} p(\mathbf{y}_u \mid \mathbf{y}_v) &= N(\mathbf{y}_u \mid \mathbf{K}\mathbf{y}_v, \mathbf{\Gamma}_{y,uu}^{-1}) \\ &\propto \exp\left[-\frac{1}{2} (\mathbf{y}_u - \mathbf{K}\mathbf{y}_v)^T \mathbf{\Gamma}_{y,uu} (\mathbf{y}_u - \mathbf{K}\mathbf{y}_v) \right] \end{aligned} \quad (11)$$

The evidence is merely a normalizing factor, independent of $\mathbf{x}_u$. However, this conditional probability is important in damage detection to remove the environmental or operational effects, which will be discussed in Section 3.

2.3. Prior

The prior distribution $p(\mathbf{x}_u \mid \mathbf{y}_v)$ is obtained from the measurement model (2) by partitioning and conditioning. The prior mean is

$$\begin{aligned} E(\mathbf{x}_u \mid \mathbf{y}_v) &= E(\mathbf{y}_u \mid \mathbf{y}_v) - E(\mathbf{w}_u) \\ &= E(\mathbf{y}_u \mid \mathbf{y}_v) = \mathbf{K}\mathbf{y}_v \end{aligned} \quad (12)$$

and the prior covariance is

$$\begin{aligned} \mathbf{\Sigma}_{\text{prior},uu} &= \operatorname{cov}(\mathbf{x}_u \mid \mathbf{y}_v) \\ &= \operatorname{cov}(\mathbf{y}_u \mid \mathbf{y}_v) - \mathbf{\Sigma}_{w,uu} = \mathbf{\Gamma}_{y,uu}^{-1} - \mathbf{\Sigma}_{w,uu} \end{aligned} \quad (13)$$

The prior distribution is also Gaussian:

$$p(\mathbf{x}_u \mid \mathbf{y}_v) = N(\mathbf{x}_u \mid \mathbf{K}\mathbf{y}_v, \mathbf{\Sigma}_{\mathrm{prior},uu})$$
$$\propto \exp\left[-\frac{1}{2}(\mathbf{x}_u - \mathbf{K}\mathbf{y}_v)^T \mathbf{\Sigma}^{-1}_{\mathrm{prior},uu}(\mathbf{x}_u - \mathbf{K}\mathbf{y}_v)\right] \quad (14)$$

2.4. Posterior

The posterior distribution (5) is obtained by some manipulation, resulting in

$$p(\mathbf{x}_u \mid \mathbf{y}) =$$
$$c \exp\left[-\frac{1}{2}(\mathbf{x}_u - \hat{\mathbf{x}}_u)^T \mathbf{\Sigma}^{-1}_{\mathrm{post},uu}(\mathbf{x}_u - \hat{\mathbf{x}}_u)\right] \quad (15)$$

where c is a constant and the posterior covariance $\mathbf{\Sigma}_{\mathrm{post},uu}$ is

$$\mathbf{\Sigma}_{\mathrm{post},uu} = \mathrm{cov}(\mathbf{x}_u \mid \mathbf{y}) = (\mathbf{\Sigma}^{-1}_{w,uu} + \mathbf{\Sigma}^{-1}_{\mathrm{prior},uu})^{-1} \quad (16)$$

and the posterior mean is

$$\hat{\mathbf{x}}_u = E(\mathbf{x}_u \mid \mathbf{y})$$
$$= \mathbf{\Sigma}_{\mathrm{post},uu}(\mathbf{\Sigma}^{-1}_{w,uu}\mathbf{y}_u + \mathbf{\Sigma}^{-1}_{\mathrm{prior},uu}\mathbf{K}\mathbf{y}_v) \quad (17)$$

The expected value of the posterior probability density function (PDF) is chosen for the virtual sensor reading. The statistical data analysis proceeds as usual, except that now the actual measurements are replaced with the virtual sensors.

3. Damage Detection

A single vibration measurement period is relatively short, and can be assumed to take place at constant environmental conditions. Environmental or operational variations occur between measurements. Their effects can be taken into account by building a covariance matrix using several measurements from the undamaged structure under different environmental or operational conditions.

Using the conditional probability $p(x_u|\mathbf{x}_v)$, each virtual sensor under variable environmental conditions can be estimated using the other virtual sensors in the network. For actual sensors (raw data), the corresponding conditional probability is $p(y_u|\mathbf{y}_v)$ [4]. The mean of the conditional probability (9) is often more accurate than the mean of the variable. This is illustrated in Fig. 1 showing two variables, both of which are influenced by a latent variable so that their standard deviations are large (black PDFs). The conditional PDFs $p(y_1|y_2)$ and $p(y_2|y_1)$ are shown in red after a data point (red circle) is observed. Their standard deviations are smaller. Consequently, the environmental or operational influences can be eliminated by replacing the variable means with the conditional means.

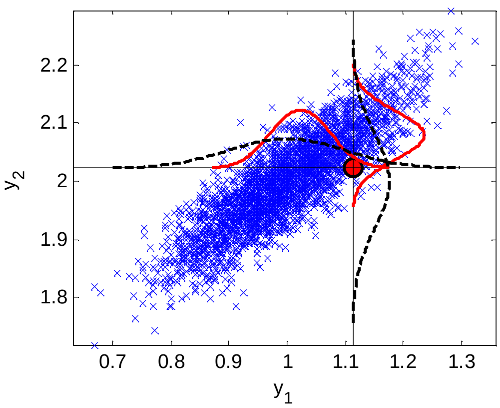

Fig. 1. An example of conditional probability distributions (red). The red circle is an observed data point.

A residual vector is then generated:

$$\boldsymbol{\varepsilon}_u = \mathbf{y}_u - E(\mathbf{y}_u \mid \mathbf{y}_v) \quad (18)$$

where $\mathbf{y}$ can be either the actual measurement or the virtual sensor (17).

For a reliable statistical analysis, the dimensionality is reduced using principal component analysis (PCA). The damage-sensitive features are the first principal component scores of the residuals, but they may not be Gaussian. Therefore, extreme value statistics (EVS) distribution is estimated [5] to design a control chart [6] for damage detection with appropriate control limits.

4. Numerical experiment

A finite element model of a bridge deck was built to simulate noisy vibration measurements from 28 accelerometers under variable environmental and operational conditions (Fig. 2).

The length of the bridge was 30 m and the width was 11 m. The deck was made of concrete with a Young's modulus of E = 40 GPa (at temperature T = 0°C), Poisson ratio of ν = 0.15, density of ρ = 2500 kg/m^3, and thickness of 250 mm. The stiffeners were made of steel (E = 207 GPa, ν = 0.30, ρ = 7850 kg/m^3). The longitudinal stiffeners had a web with a thickness of t = 16 mm and a height of h = 1.4 m. The bottom flange had a thickness of t = 50 mm and a width of b = 700 mm. The lateral stiffeners were 1.4 m high and 30 mm thick plates.

The nodes of the bottom flanges were simply supported at both ends of the bridge. Longitudinal displacements were fixed only at one end of the bridge. The corners of the concrete deck were supported in the lateral and vertical directions.

The deck was affected by temperature variability. The ends of the bridge were at random temperatures between –20°C and +40°C, and the temperature distribution was linear in the longitudinal direction and constant in the lateral direction. The temperature in each cross-section had some variation having a standard deviation of 0.2°C. The Young's modulus of concrete had a stepwise linear relationship with temperature. Different realizations of the Young's modulus is shown in Fig. 3. The temperature or the Young's moduli were not measured.

Two independent random loads in the vertical direction were applied at the nodes shown as green dots in Fig. 2. A steady state response was assumed.

The response was computed with a modal superposition algorithm using the first seven modes. The analysis period was 20.48 s with a sampling frequency of 50 Hz. One measurement period then included 1024 samples from each sensor.

Same amount of Gaussian noise was added to all sensors. The average signal-to-noise ratio of the sensor array was 40 dB. For the corresponding virtual sensors, the average signal-to-noise ratio increased to almost 48 dB.

Damage was a crack with an increasing size in a longitudinal steel girder. Six different crack configurations were modelled with an increasing severity by removing the contact between elements at 1–6 nodes. The nodes are shown in the detailed plot in Fig. 4 showing the order in which the nodes were separated. Each damage scenario was monitored with three measurements under random environmental and operational conditions. As a result, the last 18 measurements were from a damaged structure.

50 measurements were acquired from the undamaged structure under random environmental conditions. The training data were the first 25 measurements. They were also used to design the control charts. Test data were the last 43 measurements, from which the last 18 were from the damaged structure.

Damage detection was visualized with an EVS control chart, designed for the first principal component scores of the residual vector with a subgroup size of 100 samples. A generalized extreme value distribution was identified, and the PDFs of the minima and the negative maxima are plotted in Figs. 5 and 6 together with the corresponding histograms. It can be seen that the probability distributions were correctly identified. Damage detection using the actual measurements and the virtual sensors are shown in Figs. 7 and 8, respectively. With the raw measurements, only the largest crack size could be detected, whereas with the virtual sensors, the four largest crack sizes were detected. There were no false alarms when using the actual measurements (Fig. 7) and one false alarm using the virtual sensors (Fig. 8).

Damage was assumed to locate in the vicinity of the sensor u with the largest Mahalanobis distance [3] of the residual (Eq. 11). The Mahalanobis distances of the residuals for each sensor are plotted in Fig. 9. Damage was localized to sensor 11 that was indeed the nearest sensor from the crack (Fig. 2).

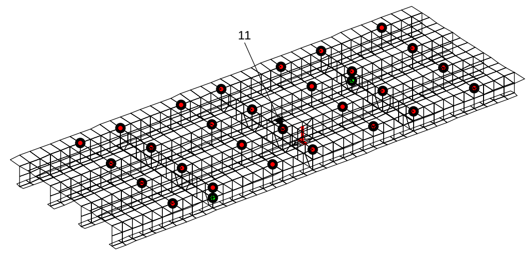

Fig. 2. Finite element model of the bridge deck. The sensor network is shown with red dots. Excitation locations are the two green dots, and the crack in a girder is plotted in red.

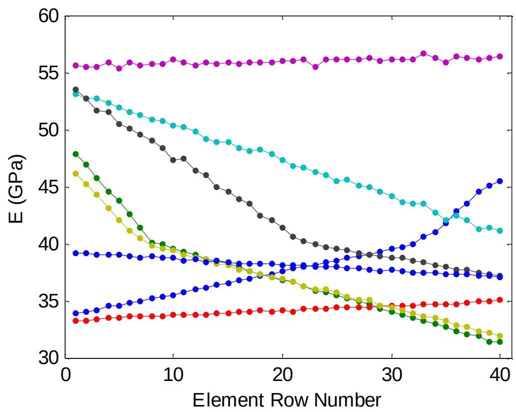

Fig. 3. Eight realizations of the longitudinal distributions of the Young's modulus of the concrete.

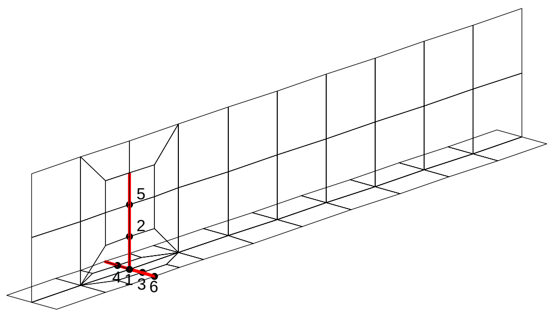

Fig. 4. A detail of the girder with damage. The crack is shown with red lines and the numbers indicate the order in which the connecting nodes separated to form an increasing crack size.

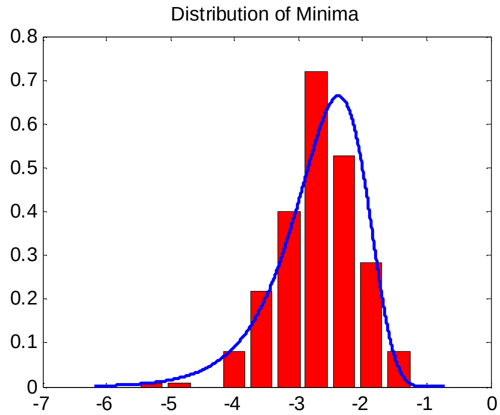

Fig. 5. Histogram and estimated PDF of the minima of the first principal component scores of the residuals in the training data.

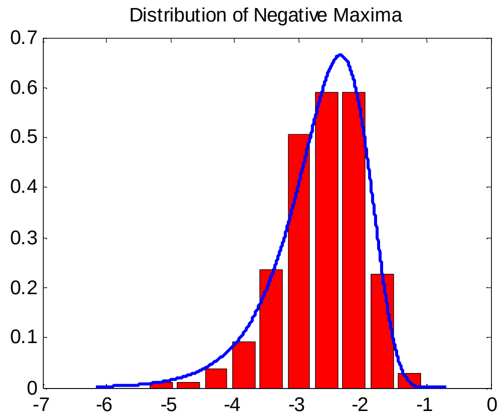

Fig. 6. Histogram and estimated PDF of the negative maxima of the first principal component scores of the residuals in the training data.

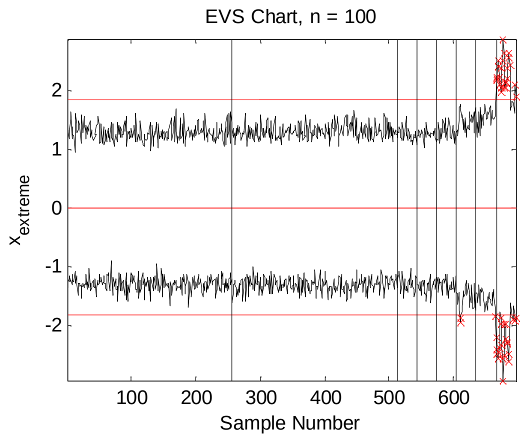

Fig. 7. EVS control chart using raw measurements. The six different damage levels are separated with the vertical lines in the right. The training data are to the left of the first vertical line.

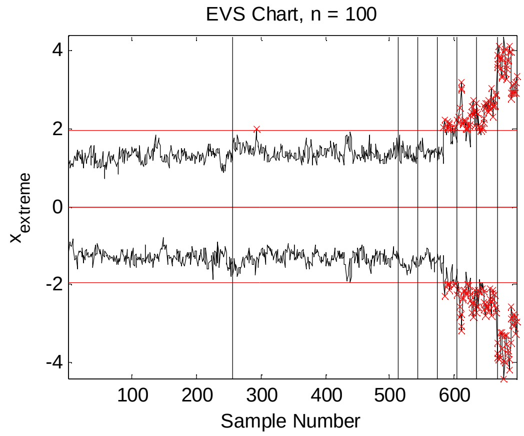

Fig. 8. EVS control chart using virtual sensors.

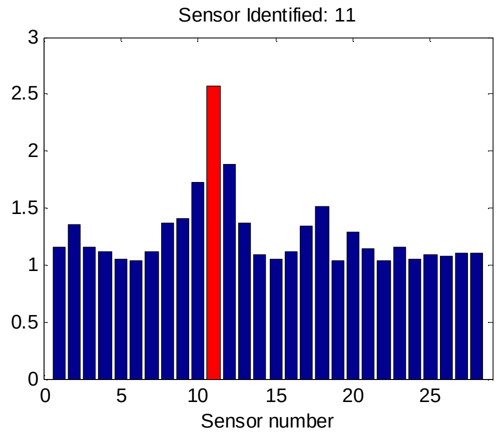

Fig. 9. Damage localization using virtual sensors.

5. Conclusions

With an increasing number of sensors, the measurement error can be reduced using Bayesian virtual sensors replacing the actual measurements and resulting in a better damage detection performance. Noise reduction was made for each measurement individually, while the environmental or operational influences were removed using all training data.

It should be noted that the proposed method was based solely on the response data, and no finite element model was used. Because damage detection was made in the time domain, no complex system identification was needed. The excitation was random and unknown. In addition, the environmental variables were not available.

Acknowledgements

This research has been supported by Metropolia University of Applied Sciences.

References

[1]. J. Kullaa, Bayesian virtual sensing in structural dynamics, *Mechanical Systems and Signal Processing*, Vol.115, 2018, pp. 497–513.

[2]. J. Kullaa, Sensor validation using minimum mean square error estimation, *Mechanical Systems and Signal Processing*, Vol. 24, 2010, pp. 1444–1457.

[3]. C.M. Bishop, Pattern recognition and machine learning, New York, *Springer*, 2006.

[4]. J. Kullaa, Eliminating environmental or operational influences in structural health monitoring using the missing data analysis, *Journal of Intelligent Material Systems and Structures*, Vol. 20, Issue 11, 2009, pp. 1381–1390.

[5]. K. Worden, D. Allen, H. Sohn, C.R. Farrar, Damage detection in mechanical structures using extreme value statistics, in *SPIE Proceedings, Vol. 4693, 9th Annual International Symposium on Smart Structures and Materials*, San Diego, CA, 2002, pp. 289–299.

[6]. D.C. Montgomery, Introduction to statistical quality control, 3rd edition, New York, *Wiley*, 1997.